Journal of Plant Research (2018) 131:319–329
https://doi.org/10.1007/s10265-017-0986-5

REGULAR PAPER

Molecular characterization of cytosolic cysteine synthase in *Mimosa pudica*

Md. Harun-Ur- Rashid[1,5] · Hironori Iwasaki[3] · Shigeki Oogai[1] · Masakazu Fukuta[2] · Shahanaz Parveen[1,5] · Md. Amzad Hossain[2] · Toyoaki Anai[4] · Hirosuke Oku[3]

Received: 16 August 2017 / Accepted: 21 September 2017 / Published online: 27 November 2017

Abstract

In the cysteine and mimosine biosynthesis process, *O*-acetyl-L-serine (OAS) is the common substrate. In the presence of *O*-acetylserine (thiol) lyase (OASTL, cysteine synthase) the reaction of OAS with sulfide produces cysteine, while with 3-hydroxy-4-pyridone (3H4P) produces mimosine. The enzyme OASTL can either catalyze Cys synthesis or both Cys and mimosine. A cDNA for cytosolic OASTL was cloned from *M. pudica* for the first time containing 1,410 bp nucleotides. The purified protein product from overexpressed bacterial cells produced Cys only, but not mimosine, indicating it is Cys specific. Kinetic studies revealed that pH and temperature optima for Cys production were 6.5 and 50 °C, respectively. The measured Km, Kcat, and Kcat Km^{-1} values were 159 ± 21 µM, 33.56 s^{-1}, and 211.07 $mM^{-1}s^{-1}$ for OAS and 252 ± 25 µM, 32.99 s^{-1}, and 130.91 $mM^{-1}s^{-1}$ for Na_2S according to the *in vitro* Cys assay. The Cy-OASTL of *Mimosa pudica* is specific to Cys production, although it contains sensory roles in sulfur assimilation and the reduction network in the intracellular environment of *M. pudica*.

Keywords α-Aminoacrylate · Cysteine · 2,5-Dimethyl-3-pyridinol · *O*-acetylserine (thiol) lyase · Mimosine

Introduction

Cysteine (Cys) is one of the reduced sulfur sources (Birke et al. 2015) and the unique access pathway for reduced sulfur (Wirtz et al. 2012) in plants. It has a cross link with trace element exposure and maintains the sulfur homeostasis (Na and Salt 2011) by upregulating the activities of S-assimilating enzymes (Lafaye et al. 2005). In plants, an unusual amount of sulfide is produced, in contrast with that of animals, in the S-assimilation pathway (Takahashi et al. 2011). Sulfide is suspected to be a substrate, toxin, and signal molecule considering its roles in the plant life cycle (Birke et al. 2015).

Plants uptake sulfate from the soil through their root channels by specific sulfate transporters (SULTRs) (Buchner et al. 2004). The formation of adenosine 5′-phosphosulfate (APS) by ATP sulfurylase (ATPS) is an important branching point of this pathway. APS is then turned into sulfite, subsequently to be reduced to sulfide by the following two enzymatic reactions using APS reductase (APR) and ferredoxin dependent sulfite reductase (SiR). Sulfate reduction usually occurs in the chloroplasts in green plants, except *Euglena gracilis* (Heeg et al. 2008), and only ATPS is localized in the cytosol (Renosto et al. 1993).

Cys biosynthesis is solely dependent on the rate of OAS supply (Haas et al. 2008; Wirtz et al. 2004), and Cys generation becomes inadequate because of the lack of available sulfide under sulfur limiting conditions, resulting in excess OAS accumulation (Krueger et al. 2009; Wirtz et al. 2012). An acetyl moiety from acetyl-CoA is transferred to serine by serine acetyltransferase (SAT, EC 2.3.1.30), and thus formed

Electronic supplementary material The online version of this article (doi:10.1007/s10265-017-0986-5) contains supplementary material, which is available to authorized users.

✉ Masakazu Fukuta
msfukuta@agr.u-ryukyu.ac.jp

[1] The United Graduate School of Agricultural Sciences, Kagoshima University, Kagoshima, Japan

[2] Graduate School of Agriculture, University of the Ryukyus, Okinawa, Japan

[3] Tropical Biosphere Research Center, University of the Ryukyus, Okinawa, Japan

[4] Faculty of Agriculture, Saga University, Saga, Japan

[5] Faculty of Agriculture, Sher-e-Bangla Agricultural University, Dhaka, Bangladesh

to OAS. The acetyl group of OAS is transposed via a free reduced sulfide molecule in a β-replacement reaction by the *O*-acetylserine (thiol) lyase (OASTL, EC 4.2.99.8) to invoke Cys production.

Some isozymes of OASTLs (Cys synthases) are capable of producing heterocyclic-β-substitute alanine synthase (mimosine and so on), and in these cases, OAS (donor of alanyl moiety) is considered to be a suitable intermediate (Murakoshi et al. 1972). Thus, mimosine production is activated by OASTL by the intermediate OAS and 3-hydroxy-4-pyridone (3H4P) (Fig. 1) (Ikegami et al. 1990).

SAT and OASTL are members of multigene families (Inoue et al. 1999; Saito et al. 1994) that are abundantly expressed in the plant cell (Hell and Wirtz 2008). They are connected in the demand-driven Cys biosynthesis regulatory process (Feldman-Salit et al. 2009; Wirtz et al. 2010a) by forming hetero-oligomeric Cys synthase complex (CSC) (Campanini et al. 2005; Hell and Wirtz 2008; Kumaran and Jez 2007; Saito 2004; Wirtz and Hell 2006). CSC acts as a sensor for sulfur availability in the cell (Wirtz et al. 2012). The intracellular level of sulfide and OAS connect and disrupt the CSC proportionately (Droux et al. 1998; Wirtz et al. 2004). SAT activity is elevated, whereas OASTL activity is decreased after forming the CSC, and thus impede the subsequent Cys conversion via OAS (Takahashi et al. 2011). OASTL is bolstered by the action of free and surplus mobile homodimers of OASTL present in the cell (Takahashi et al. 2011). Typically, OAS dominating CSC disorganization occurs because of sulfur starvation, as well as the management of high dictation pressure of Cys biosynthesis (Wirtz et al. 2012).

Cys formation in plants is sub-cellular compartment specific and takes place in the cytosol, plastid, and mitochondria (Heeg et al. 2008; Na and Salt 2011; Noji et al. 1998; Pilon-Smits and Pilon 2006; Saito 2000; Wirtz et al. 2010b; Watanabe et al. 2008). Amount and activity of SAT and OASTL differ significantly according to the compartment of the cell where the CSC is situated, and also the inequitable distribution of OASTL activity varies according to the amount of OASTL protein (Wirtz et al. 2010a). Approximately 90% OASTL actively occurs in the cytosol and chloroplasts, with the remainder in the mitochondria in *Arabidopsis thaliana* leaves, whereas approximately 80% of SAT activity occurred in the mitochondria (Heeg et al. 2008; Watanabe et al. 2008; Wirtz et al. 2010a). It is evident that functional diversity of OASTL is a common phenomenon in higher plants, and the highest Cys biosynthesis occurs in the cytosol and the lowest in mitochondria (Krueger et al. 2009). The precise compartment localization of SAT and OASTL occurs because of the putative nature of Cys and

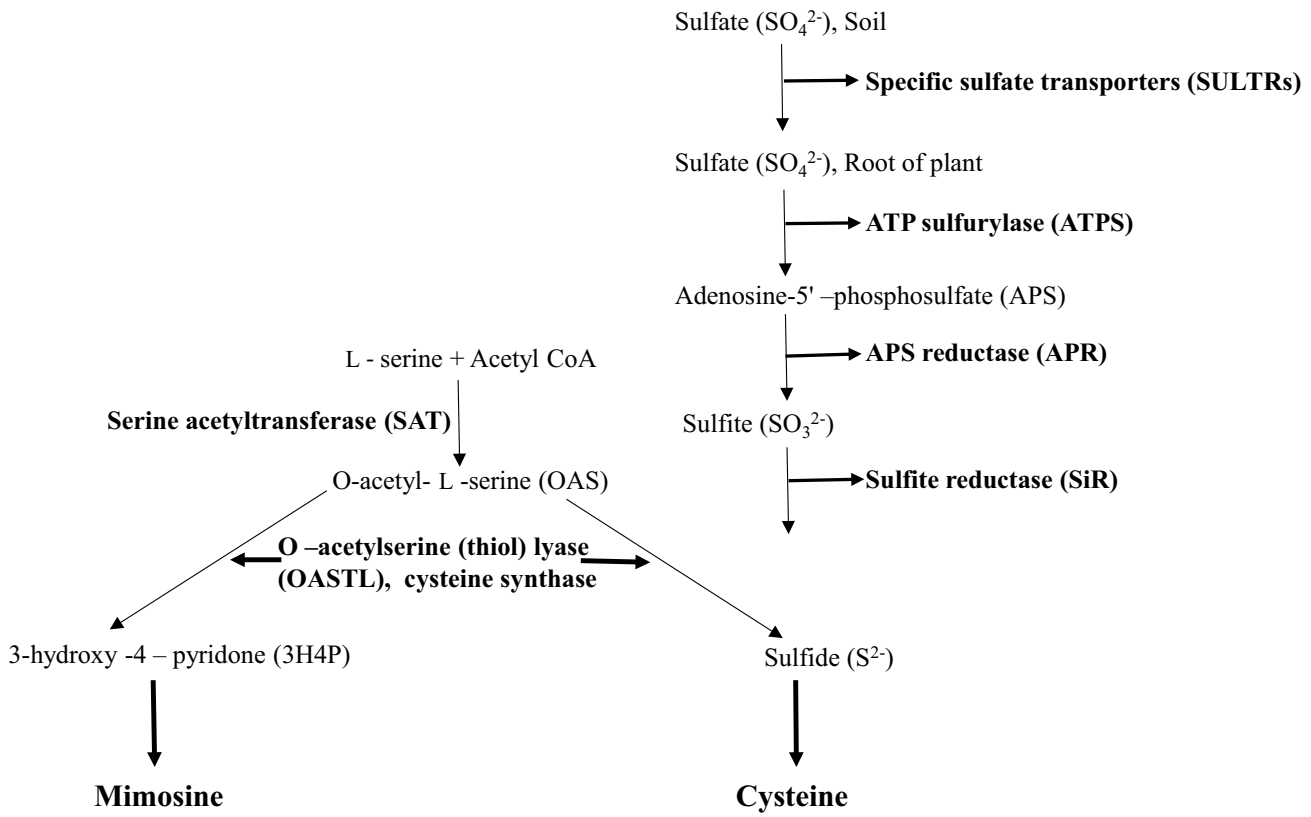

Fig. 1 Sulfate assimilation triggers S-containing standard and non-standard amino acid biosynthesis pathway in *M. pudica*

its derivatives within the compartments (Heeg et al. 2008; Watanabe et al. 2008). Conversely, the compartment specific nature of OAS and OASTL is not inherent and occurred during evolution as a result of gene duplication (Heeg et al. 2008; Watanabe et al. 2008). Thus, all OASTLs in plant cells contain unique roles for protein production, and their activities are solely dependent on their location, and the subsequent nature of protein folding and substrate affinity are related to its evolutionary aspects.

Herein, we present the first description of cloning, purification, and characterization of cytosolic OASTL from *Mimosa pudica* Mill. and its expression in *Escherichia coli* to determine the cross link between this OASTL and mimosine formation and elucidate the metabolic roles of cytosolic OASTL in *M. pudica*.

Materials and methods

Chemicals

Standard mimosine was obtained from Sigma-Aldrich, Co., USA. For the norm 3H4P preparation, standard mimosine powder (10 mg, expected final concentration 5 mM) was appended into 5 mL of 50 mM sodium phosphate buffer (pH 8.0) followed by incubation at 50 °C with periodic shaking until the mimosine completely dissolved. One-hundred microliters of 1 mM PLP was added to the solution and distilled water was added to make the final volume 9.5 mL. Then, 0.4 mg mL^{-1} recombinant *M. pudica* mimosinase (0.5 mL) was added, followed by incubation at 50 °C for 3 h with shaking. The final concentration of 3H4P in the solution was 5 mM. The proteins were removed using Amicon Ultra-4 filters Ultracel-10K. HPLC analysis confirmed complete degradation of mimosine and production of equimolar 3H4P.

RNA isolation and cDNA synthesis

A total of 100 mg of *M. pudica* leaves were frozen in liquid nitrogen and ground into powder using a sterilized mortar and pestle. As stated by the manufacturer, total RNA was extracted from the powder using the RNeasy Plant Mini Kit (QIAGEN). Poly (A+) RNAs were purified and isolated using the poly (A+) RNA Kit (Nippon Gene) following the manufacturer's direction.

RT-PCR experiments were performed using both directional degenerated primers (5′-GGNCCNGARATHTGGGARGAYAC-3′ and 3′-GNCTYTTRCGNCCNTTYRANTAD-5′) corresponding to conserved amino acid regions within the Cys synthase family available in the database to obtain candidate cDNAs, and an oligo dT primer for *M. pudica* mRNA was used as a template with the One Step RT-PCR Kit (QIAGEN). A 406-nucleotide cDNA product consisting of a deduced C-terminal 36 amino acid coding region, which appeared similar to corresponding parts of the Cys synthase family, and a putative 298 nucleotide 3′ untranslated region was obtained. The full-length cDNA sequence of the putative *M. pudica* Cys synthase was determined from the product of a 5′ RACE experiment. RACE analysis was performed with an outer (5′-CTTTCAATG CAAGATTTAGCAG-3′) and inner reverse primer (5′-TAG CTTCTTCACTGGATATCTGG-3′) with First Choice® RLM-RACE Kit (ThermoFisher Scientific).

Expression of Cy-OASTL

The PCR amplified OASTL gene was digested with EcoRI and XhoI. Furthermore, it was inserted into the expression vector pGEX6p-3 that contains a GST tag at the 5′ end using the DNA ligation kit (TAKARA BIO INC.). The expression constructs were introduced into the host bacteria *E. coli* BL 21 (DE3) pLysS containing T7 RNA polymerase for the induction of the lacUV5 promoter via isopropyl β-D-1-thiogalactopyranoside (IPTG). The transformed clone selection was made by the selection pressure carbenicillin (Cb, 50 mg mL^{-1}) on LB agar medium.

A single colony of insert DNA was pre-cultured overnight with vigorous shaking at 37 °C in LB medium with Cb (50 mg mL^{-1}). An aliquot of the preculture cells was inoculated into LB broth medium at 37 °C. IPTG was added at various concentrations (0.1 to 1 mM) at the mid-log growth phase (OD_{600} = 0.4–0.8) of the bacteria, as well as different temperatures (20–30 °C) and times (2–4 h) for the optimization of the recombinant protein expression. The harvested cells were suspended in 20 mL PBS (−) and sonicated 20 times (30 s each) in ice using a homogenizer for disrupting cell suspensions. The lysate was centrifuged at 13,200 rpm for 10 min at 4 °C to remove cell debris, and the supernatant was used as the crude recombinant protein.

The filtered crude protein was placed in the GST fusion protein purification column (GSTrap FF, GE Healthcare, Japan) for affinity purification. The GST part was separated by digestion with PreScission protease (Amersham), and the flow through fraction was used as purified recombinant protein. SDS-PAGE confirmed the purity of the recombinant protein after 3 min heating at 95 °C, which was visualized by CBB (Coomassie Brilliant Blue) staining.

Genetic complementation of cytosolic OASTL

Genetic complementation of OASTL was conducted to determine whether the gene of interest could produce Cys in the *E. coli* NK3 strain (Cys auxotroph mutant) on an M9 (minimal nutrient agar) plate without adding Cys. The recombinant plasmid (pGEX6p-3) harboring the OASTL

fused with glutathione S-transferase under the control of the tac promoter, and was isolated from the host JM109 and transformed into NK3. *E. coli* NK3 with the expression vector devoid of the gene of interest served as a negative control. NK3 with or without OASTL (empty vector) were streaked onto M9 plates supplemented with (0.5 mM Cys) and without Cys, and incubated at 37 °C overnight.

Cysteine synthesis activity measurement

Cys production activity was validated in 50 mM Tris–HCl or phosphate buffer (final pH 7.5), purified enzyme solution (equivalent 1–2 µg of protein), 2.5 mM Na_2S, 10 mM OAS, 1 mM DTT, and 0.5 mM PLP in a final volume 100 µL. Pre-incubation was performed at 30 °C for 5 min. The reaction was advanced after placing Na_2S in the reaction mixture followed by termination with the addition of 0.05 ml 20% (w/v) trichloroacetic acid (TCA). Cys absorption was measured according to Gaitonde (1967) at λ560 with the reaction output showing pink color as a Cys-ninhydrin adduct.

The Cys synthesis assay was optimized with different buffer (citric acid buffer, boric acid buffer, and $NaHCO_3$ buffer) pH (3.0–12.0), different temperatures (20–60 °C), and different concentrations of Na_2S and OAS substrates. All the assays were repeated three times at each point. A standard curve corresponding to altered levels of standard Cys (Wako Pure Chemical Industries, Ltd., Japan, 0.1–0.12 mM) determined the actual concentration of Cys by spectrophotometer. An Excel program was used to analyze the data, and non-linear regression analyses determined the Km, Kcat, and other values.

High-performance liquid chromatography (HPLC) condition for mimosine detection

A Shimadzu UFLC XR HPLC system (equipped with a quaternary pump, a vacuum degasser, a thermostatted column compartment, and an autosampler) performed the chromatographic analysis. An Inertsil ODS-3 column (4.6 mm × 150 mm) separated the sample. The mobile phase consisted of MilliQ water containing 0.1% formic acid (A) and acetonitrile (B), and a flow rate of 1 mL min^{-1} was used followed by an isocratic mode (0.0–3.0 min, 100% A; 3.0–7.0 min, 0% A). The injection volume was 1 µL for substrate 3H4P and the mimosine standard, and 5 µL for the incubated sample. Mimosine and 3H4P were detected at λ280.

Phylogenetic tree making

MEGA version 7.0 (Kumar et al. 2016) was used to build a molecular phylogenetic tree for OASTL of *M. pudica*. The neighbor joining method (Saitou and Nei 1987) was used accompanying the bootstrap value of 1000 replicates (Felsenstein 1985). Plant Cys synthase protein sequences from the database demonstrated more than 80% similarity, excluding the predicted and hypothesized sequences obtained in phylogeny computation. The total 18 amino acid sequence evolutionary distances were enumerated considering the Poisson correction method (Zuckerkandl and Pauling 1965). After removing gaps and missing data, a total of 301 positions were in the final dataset.

Bioinformatics analysis of OASTL in *M. pudica*

Measurements such as putative molecular mass, formula, and weight, and isoelectric point of the protein were determined using Protparam software (http://web.expasy.org/Portparam). ProtScale (http://web.expasy.org) was used to predict the hydrophobic and hydrophilic nature of the OASTL protein, and TMHMM server v.2.0 (http://www.cbs.dtu.dk/services/TMHMM/) was used for the prediction of transmembrane helices in the protein. SignalP4.1 server (http://www.cbs.dtu.dk/services/signal) was used to analyze the signal amino acid sequences, and ProtFun (http://www.cbs.dtu.dk/services/ProtFun) was used for the prediction of the function of OASTL protein in *M. pudica*.

Homology modelling

Cys synthase three-dimensional structure (3D) was not available in the Protein Data Bank (PDB). The T-COFFEE server was used for Cys synthase multiple sequence alignment. Based on the multiple sequence alignment data, the putative model of Cys synthase was generated using the MODELLER ver.9.16 software from the crystal structure of *A. thaliana O*-acetylserine sulfhydrylases (PDB ID 1z7w) as a template.

MODELLER was run with the following parameters: library_schedule, max_var_iterations, 300; autosched.slow; md_level, refine; very slow; and repeat_optimization, 10 (Scharer et al. 2011). Out of the models, the 10 best generated OASTL models were used for docking simulations with OAS followed by the best OASTL-OAS complex selection considering the highest binding energy plus the maximum population in one cluster.

Docking simulation

Parameter files were generated by the AutoDockTools 1.5.6 for docking simulation. Before docking simulation, OASTL protein and substrate OAS, PDB files converted to the AutoDock type format (PDBQT) along with the addition of a Gasteiger charge to each atom.

AutoDock 4.2 was deployed for docking simulation (100 GA runs) using the Lamarckian genetic algorithm and

a confined grid size (50×50×50) using Autogrid (spacing of 0.375 Å). The docking parameters are as follows: translation step size, 2 Å; torsion step size, 50 °C; number of individuals in population, 150; maximum number of energy evaluation, 25,000,000; rate of gene mutation, 0.02; rate of crossover, 0.8; GA crossover mode, twopt; and elitism, 1.

Inter-fragment interaction energy (IFIE) calculation

Ligand and receptor protein inter-fragment interaction energy was calculated with the PAICS program (Ishikawa et al. 2009) using the fragment molecular orbital (FMO) method (Kitaura et al. 1999a, b). The large protein molecule was divided into small pieces to calculate the interaction between substrate and enzyme by the FMO method. The AMBER program energy minimized the ligand-receptor complex (Ponder and Case 2003) that was used in the PAICS program input file generation.

Results

Cysteine synthase cloning and expression

The isolated OASTL full-length cDNA sequence (accession number BAK 38374) was 1,410 bp in length revealing an open reading frame of 987 bp encoding 329 amino acids. The predicted molecular weight of the protein was 34.72 kDa, which agreed well with the SDS-PAGE (Fig. S1). The expressed protein molecular weight was 60.72 kDa (with GST-tag), whereas the purified protein was 34.72 kDa (Fig. S1). Protein subcellular localization prediction software (http://wolfpsort.hgc.jp) suggested that the cloned OASTL of *M. pudica* is localized in the cytoplasm, so we referred to it as "Cy-OASTL."

HHpred detection software (http://toolkit.tuebingen.mpg.de/hhpred) denoted that Cy-OASTL is PLP dependent and classified under transferase category. A phylogenetic tree of *M. pudica* Cy-OASTL demonstrated the highest identity (89%) with the Cys synthase sequence of *Phaseolus vulgaris* (AGV54667, Fig. S3 and Table S1). The phylogenetic data also asserted that Cy-OASTL of *M. pudica* was unique.

Genetic complementation test

To confirm the ability of Cys production by Cy-OASTL, a genetic complementation test was conducted using *E. coli* NK3. NK3 with recombinant plasmid grew on the Cys lacking M9 plate, whereas the *E.coli* NK3 (empty vector) was unable to develop (Fig. 2). These difference in growth indicated that Cy-OASTL indeed a functionally active Cys synthase.

Cysteine synthase assay

The effects of pH, reaction temperature, and substrates (OAS and Na_2S) on Cys synthase kinetic properties were studied by varying the parameters. The pH range 5.0–6.5 consistently increase Cys synthase activity, which abruptly declined at pH ≥ 7.0 (Fig. 3a). Cys synthase activity was nearly deactivated at pH ≥ 10.0. Cy-OASTL of *M. pudica* revealed its preference for pH 6.5 by demonstrating that a nearly neutral pH environment created a positive atmosphere for the activity of this enzyme (Fig. 3a).

The highest catalytic activity of Cys synthase was at 50 °C (Fig. 3b) and was considered the ideal temperature for Cy-OASTL. Activity was gradually increased between 20 and 50 °C and sharply declined at 55 °C (Fig. 3b).

The Km value of Na_2S was higher than the OAS. The Km value of Na_2S and OAS was 252 ± 25 µM sulfide and 159 ± 21 µM OAS (Table 1), whereas the Kcat value of OAS

Fig. 2 Functional genetic complementation of the cysteine auxotroph *E. coli* NK3. The bacteria were spread on the M9 minimal plate with 0.5 mM cysteine (left) and without cysteine (right). (1) JM109 (positive control); (2) pGEX6p-3+ NK3 (empty vector, negative control); (3) pGEX6p-3+ cytosolic OASTL + NK3

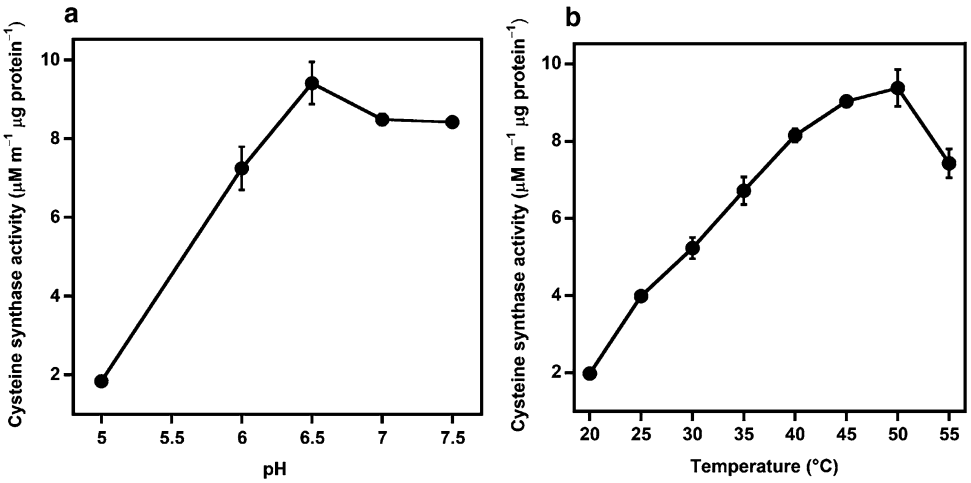

Fig. 3 pH (different buffer pH at 50 °C) (**a**) and temperature (pH 6.5) (**b**) optima of *M. pudica* Cy-OASTL for cysteine synthesis. 50 mM buffers containing 10 mM OAS, 1 mM DTT, 0.5 mM PLP, and 2.5 mM Na_2S. Data are mean ± SE ($n = 3$)

Table 1 Enzyme kinetics of cysteine synthase obtained from the cytosol of *M. pudica*

Substrate Name	Km (μM)	Kcat (s^{-1})	Kcat Km^{-1} ($mM^{-1}s^{-1}$)
OAS	159 ± 21	33.56	211.07
Na_2S	252 ± 25	32.99	130.91

*All values are expressed as a mean ± SE ($n = 3$)

and Na_2S was nearly the same being 33.56 and 32.99 s^{-1}, respectively (Table 1).

Mimosine synthesis assay

To ascertain whether *M. pudica* Cy-OASTL could produce mimosine, we performed experiment with OAS and 3H4P. Mimosine production was monitored using LC/MS. The retention time of synthetic mimosine and the substrate 3H4P standard was 1.68 min (Fig. S2-a) and 2.03 min (Fig. S2-b), respectively. OASTL, which synthesized mimosine, was considered the positive control (Fig. S2-c). The reaction mixture of the Cy-OASTL under the similar assay conditions failed to produce mimosine (Fig. S2-d). The protein with GST and without GST showed no differences in the reaction product. Thus, this result suggests that the cloned Cy-OASTL from *M. pudica* was exclusively capable of Cys production, not mimosine.

In silico characterization of OASTL in *M. pudica*

The predicted molecular formula of Cy-OASTL is $C_{1548}H_{2530}N_{412}O_{462}S_{13}$ (total number of atoms 4,965) with an isoelectric point of 6.48. Theoretically, the estimated half-life of the protein was 30 h (mammalian reticulocytes, in vitro) whereas; > 20 h (yeast, in vivo) and > 10 h (*E. coli*, in vivo) and the instability index 32.91 considering that it is a stable protein (> 40 denotes a potentially unstable protein).

Regarding the relative content of the amino acids, alanine was highest (37, 11.2%), followed by glycine (36, 10.9%) and leucine (31, 9.4%). Tryptophan (2, 0.6%) was the lowest preceded by cysteine (3, 0.9%) and histidine (4, 1.2%). The total number of negatively charged residues was 37 (Asp + Glu) compared to the 36 positives (Arg + Lys) in the Cy-OASTL protein. The aliphatic index of the protein was 101.16 based on the relative volume occupied by the aliphatic side chains, alanine, valine, isoleucine, and leucine indicating thermostability of the globular protein. The grand average of hydropathicity was 0.08. The Cy-OASTL extinction coefficient was observed at 23,045 $M^{-1}cm^{-1}$ and 22,920 $M^{-1}cm^{-1}$ (λ280 and water, respectively) corresponding to the absorbance 0.664 (all pairs of Cys residues from cystines) and 0.660 (all Cys residues in reduced form).

Predicted hydrophilic and hydrophobic nature of the OASTL protein using ProtScale, the maximum (3.011) and the minimum (− 2.389) scores were observed in valine (301 sites) and glutamic acid (198 sites) of the polypeptide chain, indicating these sites had the weakest and strongest tendency for hydrophilicity, respectively (Fig. S4). The hydrophobic region was comparatively larger than the corresponding hydrophilic region, indicating the predominant hydrophobic nature of the polypeptide chain.

According to the TMHMM server data, it was demonstrated that the OASTL protein was located outside the cell membrane. Thus, no membrane domain was present (Fig. S5). The results of DNASTAR showed that α-helices were one of the predominant secondary structures of the Cy-OASTL.

Signal P-4.1 server showed that the OASTL protein might be free from any signal peptide (Fig. S6). All the scores were near the negative target value of 0.1 indicating that the OASTL was a non-secretary protein in nature. Thus, combining with the findings of transmembrane segment

analysis, it could be concluded that the OASTL protein was directly evolved in the cytoplasm. Gene ontology category confined it as a structural protein. Also, it was devoid of the signal peptide cleavage site, propeptide cleavage site, *N*-glycosylated site, and transmembrane helices, but it contained 38 putative phosphorylation sites and 52 putative *O*-glycosylated sites.

Docking simulation of Cy-OASTL

Ten Cys synthase putative homology models were generated by MODELLER (var.9.16). We docked the *M. pudica* Cy-OASTL receptor with the ligand OAS (Fig. 4a). From the *M. pudica* Cy-OASTL-OAS complex, the model containing the highest population and highest binding energy was procured and considered for the calculation of interaction pattern between the substrate and ligand.

The receptor (Cys synthase) and ligand (OAS) molecular interaction pattern was analyzed using the FMO method (Kitaura et al. 1999a, b), and IFIE was calculated. The internal Schiff base was divided into three parts, Lys 49, 2,5-dimethyl-3-pyridinol (DMP) and phosphate (Fig. 4b), for obtaining the unambiguous result of PAICS calculation. The binding energy between the receptor and ligand was −57.585 kcal mol^{-1} and the distance was 1.83 Å.

Four amino acids, Gly 79, Gln 150, Ser 78, and Met 128, were less than 3Å away from the active site and displayed a higher attraction force. Within a 3Å distance amino acid Ile 229 provided by the highest repulsion force (Table 2; Fig. 4a).

Table 2 Inter-fragment interaction energy of attraction and repulsion force between substrate (OAS) and enzyme (cytosolic cysteine synthase) obtained by FMO methods (PAICS)

Fragment	Energy (kcal mol^{-1})	Distance (Å)
Attraction force		
Gly 79	−15.787	2.37
Gln 150	−11.925	2.25
Ser 78	−10.377	1.83
Met 128	−7.971	2.74
Phosphate	−7.866	4.68
Repulsion force		
DMP	6.728	2.70
Ile 229	2.839	2.96

Discussion

Isolated and purified bacterially expressed Cy-OASTL of *M. pudica* can produce Cys only. It could not produce mimosine under the test conditions (Fig. S2), and thus we considered it Cys specific.

The Cy-OASTL of *M. pudica* with the GST tag showed poor Cys synthase activity compared to the tag removed purified enzyme. The SDS-PAGE results revealed that the purified protein contained a single band with the suitable size (34.72 kDa) (Fig. S1). For the Cys and mimosine biosynthesis process, the first substrate, OAS, is standard but the second substrate is different (Na_2S for Cys

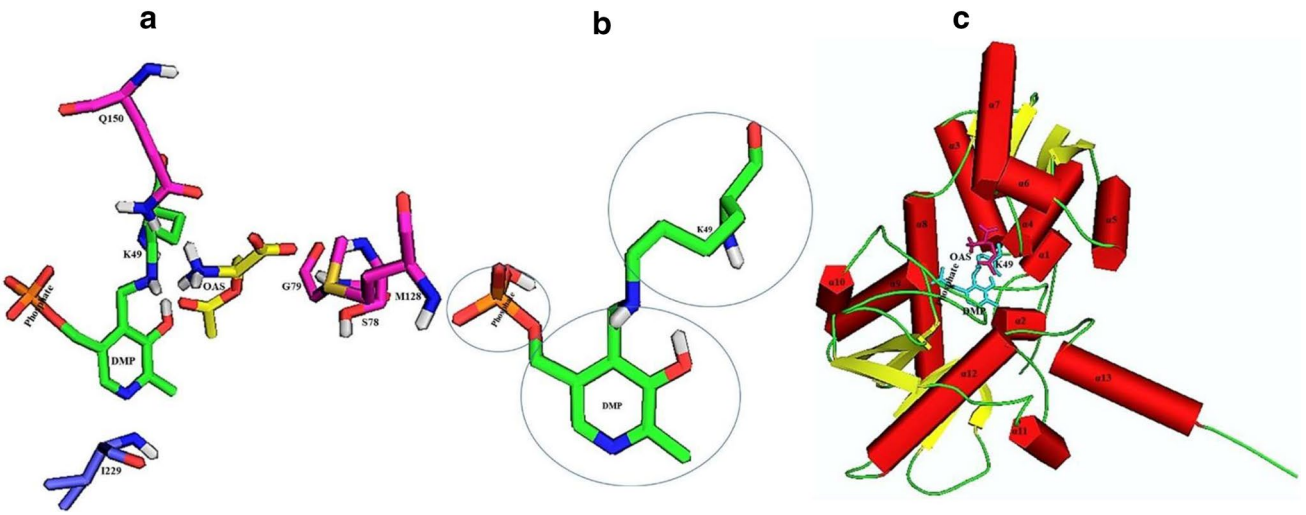

Fig. 4 Three-dimensional structure of the active site of cysteine synthase (OASTL) from *M. pudica* with ligand OAS. **a** Coordination geometry of amino acids at the active site of OASTL is shown in stick form. The carbon skeleton along with the attraction and repulsion force amino acids listed in Table 2 shown in magenta and blue, respectively. Carbon frame of Lys 49-PLP (internal Schiff base) in green and the substrate OAS shown as yellow sticks. **b** The active site of Cy-OASTL (internal Schiff base) divided into three parts for PAICS calculation, including Lys 49, DMP ring, and phosphate. **c** α-helix surrounded by the active site of Cy-OASTL. All figures were generated by PyMol

and 3H4P for mimosine) (Fig. 1). We predicted that our OASTL possessed dual functions to produce both Cys and mimosine. *In vitro* results suggest that the Cy-OASTL of *M. pudica* has only Cys synthase ability. We repeated the mimosine synthase assay several times while changing the test conditions, and also the concentration of enzymes and substrates, but no change was noticed in the HPLC results (Fig. S2). This result demonstrated that the Cy-OASTL of *M. pudica* is exclusively capable of Cys production, not mimosine. Our finding is in agreement with the results of Yafuso et al. (2014). Their cytosolic OAS-TL of *Leucaena leucocephala* also demonstrated only Cys synthase activity.

The pH and temperature optima for Cys production were 6.5 and 50 °C, respectively (Fig. 3). It may be considered that *M. pudica* Cy-OASTL is adapted to against robust daytime high temperature of tropical and subtropical climatic condition and as a result, the Cys production is favored by the temperature 50 °C. The Cy-OASTL of *L. leucocephala* (Rashid et al. under review) demonstrated ideal pH and temperature for Cys was 7.5 and 40 °C, respectively. The Km value of the Cy-OASTL of *M. pudica* was 159 ± 21 μM for OAS and 252 ± 21 μM for sulfide (Table 1). The Cy-OASTL of *L. leucocephala* (Cys specific, Yafuso et al. 2014) was Km 1,850 ± 414 μM sulfide, which is seven times greater than that of the *M. pudica* Cy-OASTL. Variations in the Km value of each enzyme demonstrates its efficiency to meet the substrates in the active site location of the protein. We observed that the elevated level of OAS suppressed Cys activity as a consequence of the lower pH in the reaction mixture (Kuske et al. 1994). These findings are in full agreement with a previous study (Warrilow and Hawkesford 2000).

All PLP-dependent enzymes retained ubiquitous three-dimensional folds in the structure (Burkhard et al. 2000; Claus et al. 2005; Ngo et al. 2007; Simanshu et al. 2006). The active site structure of the enzymatic reaction was associated with the PLP position. The PLP forms internal Schiff base with Lys (Fig. S7) in a comprehensive manner that harbors multiple interactions in the active site (Bonner et al. 2005; Yi et al. 2012). Thus, PLP position is conserved across the BSAS (β-substituted alanine synthase) family members that provide the unique gateway for reaction chemistry, albeit each enzyme favors its representative substrate (Fig. 5).

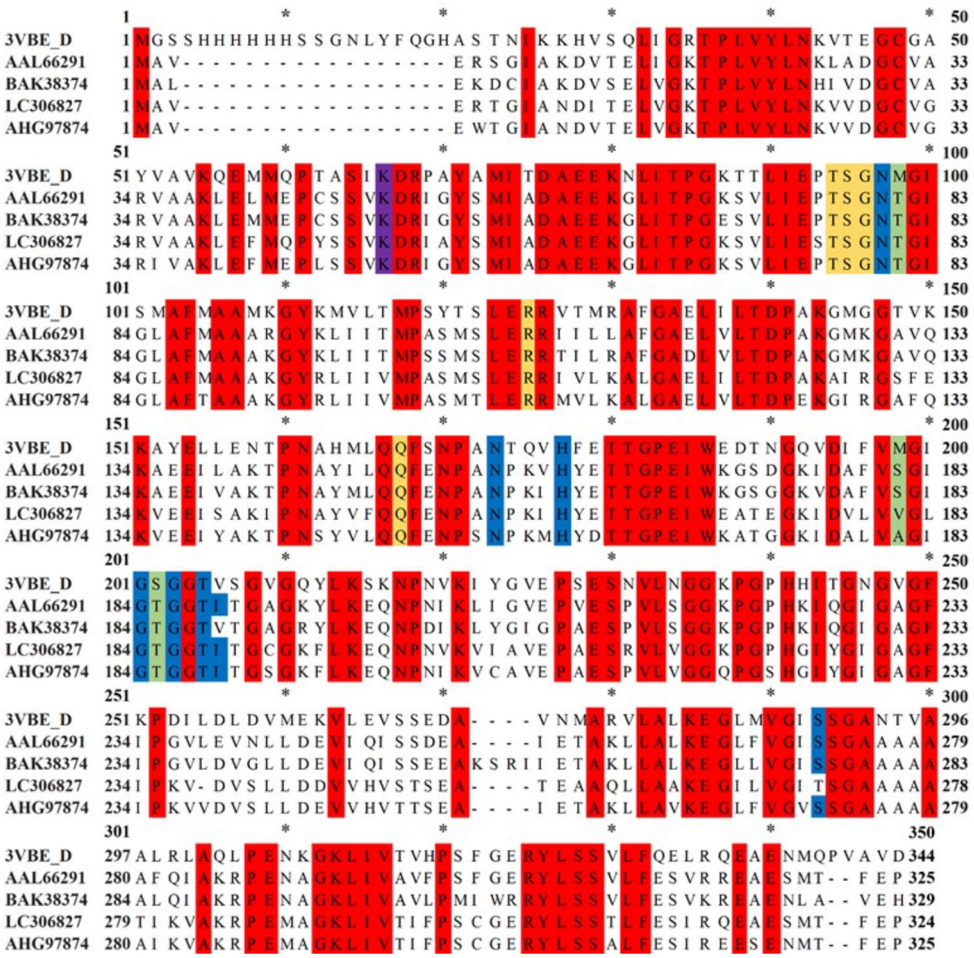

Fig. 5 Comparison of amino acid sequences among β-cyanoalanine synthase in *Glycine max* (3VBE_D), cysteine synthase in *G. max* (AAL66291), Cy-OASTL in *M. pudica* (BAK38374), Cy-OASTL in *L. leucocephala* (LC306827), and Cy-O-acetylserine thiol lyase in *L. leucocephala* (AHG97874). The amino acid residues highlighted in red show the conserved region, residues interacting with the PLP or substrate in the active site are highlighted in yellow and blue, respectively. The Lys 49 (BAK38374) that forms the internal Schiff base with the cofactor PLP is indicated in the violet

The BSAS family members, such as CAS (β-cyanoalanine synthase) and OASTL, demonstrate a common phenomenon in their respective reaction mechanisms. This response mechanism firstly involves active α-aminoacrylate intermediate generation followed by the corresponding product development with the appropriate substrate molecule, without hampering notable deviation of the non-reactive PLP-Lys external aldimine compound (Yi et al. 2012). Thus, it is an accepted view that the reaction will proceed after generation of the α-aminoacrylate intermediate with Lys from different substrate moieties.

The PLP-dependent enzyme reaction is guided by the altering open and closed conformational changes occurring in the protein structure. In the case of the Cy-OASTL in *M. pudica*, OAS would react with the C4′ of the PLP-Lys 49 (Fig. 4, Fig. S7) and release the Lys 49 residue. The α-aminoacrylate intermediate generation allows α, β-elimination of acetate from OAS by Lys 49 (Bonner et al. 2005; Burkhard et al. 2000; Tai and Cook 2006). Binding of OAS to the PLP-Lys 49 operates the position change (N-terminal domain shifting) in the substrate binding loop (TSGN) (Fig. S8). This domain regulates conformational shifts in the active site structure (open to closed conformation) of the enzyme and constrains the second substrate entrance. This conformational change in the active site allocates steric gate to restraint nucleophile entrance to the active α-aminoacrylate intermediate (Yi et al. 2012).

Lys 49 and the amino acids held by the PLP binding site are highly conserved in BSAS family members (Fig. 5). In PLP-Lys 49, Asn 80, and Ser 276 would form a hydrogen bond with the oxygen and nitrogen in the pyridine ring, respectively, and the phosphate moiety would construct hydrogen bonds among Gly 184, Thr 185, Gly 186, and the side chain hydroxyl group of Thr 185 and Thr 188 (Fig. S9). The side and main chain atoms of Thr 77, Ser 78, Gly 79, and Asn 80 (TSGN loop) construct hydrogen bonds with the carboxylate group of OAS (Fig. S8), and thus the Cys reaction scheme would proceed. Docking simulation results suggested that Gln 150 and DMP (Table 2) had a significant role in the Cys biosynthesis process.

Across the CAS and OASTL proteins, three amino acids showed variations (Fig. 5; Met 98 to Thr 81; Met 198 to Ser 181; Ser 202 to Thr 185) close to PLP-ligand (Yi et al. 2012). Their point mutation results demonstrated that additional changes are required in the active site structure around the PLP molecule for the better catalytic efficiency CAS and OASTL albeit they formed active α-aminoacrylate intermediate instead of nonreactive external aldimine (Eliot and Kirsch 2004).

BSAS enzyme requires three sequences to perform its functions, such as binding of the first ligand to the receptor, generation of active intermediate (α-aminoacrylate) with the interaction of substrate, and lastly nucleophilic attack of this active intermediate to the second ligand. Thus, in the mimosine biosynthesis reaction scheme of the Cy-OASTL, the last sequence of the enzyme might not be fulfilled. Thus, the Cy-OASTL of *M. pudica* (BAK38374) is only Cys specific. On the other hand, one of our Cy-OASTL of *L. leucocephala* (LC306827), which have dual functions for Cys and mimosine production, unlike another Cy-OASTL of *L. leucocephala* (AHG97874, Yafuso et al. 2014) that is only Cys specific. Comparing with these three sequences (Fig. 5), we found that Val 181 (LC306827) corresponded to position Ser 181 (BAK38374) and Ala 181 (AHG 97874) and Thr 271 (LC306827) to the Ser 276 (BAK38374) and Ser 272 (AHG97874). Yi et al. (2012) suggested that Thr 81, Ser 181, and Thr 185 have a predominant role in the reaction mechanism of OASTL. Divergent amino acids in the corresponding positions might be one reason for its inability to produce mimosine. In Cy-OASTL of *M. pudica*, PLP-Lys 49 complex could produce the active α-aminoacrylate intermediate with the first substrate OAS, but when the second substrate 3H4P is bound to it, it might be unable to stabilize the active structure of the α-aminoacrylate intermediate, and thus the reaction mechanism is inactive at this point and it cannot synthesize mimosine.

In the case of Cy-OASTL *M. pudica*, we used Na_2S as the second substrate for Cys and 3H4P for mimosine production. The Na_2S molecular weight is 78.04, whereas 3H4P is 112.01. The 3H4P is approximately two times larger than Na_2S. The conformational change (open to closed) occurs in the active site structure of the enzyme after reacting with OAS. This closed conformation structure of protein permits limited access of the second substrate compared to the open. As such, in the closed conformation, enzyme structure could readily allow the small molecule Na_2S, rather it hinders the entrance path for the large molecule 3H4P, or it will change the PLP anchoring amino acid environment near the active site structure, and thus the Cy-OASTL of *M. pudica* is inadequate to satisfy the BSAS family members demand for product generation, and as a result unable to synthesize mimosine.

For Cys synthesis, it is necessary to form a multi-enzyme complex (Cys synthase complex, CSC) with the association of SAT and OASTL (Fig. 1). This complex plays a vital role in controlling the Cys metabolic process. CSC could be used as a molecular sensor for the sulfate assimilation pathway and to adjust intracellular Cys magnitude (Fig. 1). SAT and OASTL play proportionate roles in the CSC, such that an increasing trend in SAT will impose a decreasing trend on OASTL, and thus it generates the OAS. Intracellular sulfur scarcity promotes excess OAS accumulation in the cell because of the sulfide paucity to form Cys with OAS and sulfide. Extra OAS detach from the enzymatic complex, and consequently the elevated concentration of OAS switch on

sulfate transporter genes. This phenomenon has a great effect as a sulfate uptake and reduction mechanism for plants.

It is evident that there are multiple copies of OASTLs in plants. All the plant OASTLs demonstrate distinct features. Cy-OASTL of *M. pudica* is only Cys specific, but it contains some unique features for the sulfate assimilation regulatory network and plays a sensory role in the cell. Furthermore, site directed mutagenesis considering the structural and molecular point will provide us with new insights regarding Cy-OASTL in the Cys biosynthesis process and sulfate assimilation network in plants.

Accession numbers

The data of protein sequences can be found in Gene bank under the following accessions: CAA58893 (Cysteine synthase, *Arabidopsis thaliana*), 3VBE_D (β-cyanoalanine synthase, *Glycine max*), AAL66291 (Cysteine synthase, *Glycine max*), BAK38374 (Cysteine synthase, *Mimosa pudica*), LC306827 (Cy-OASTL, *Leucaena leucocephala*), and AHG97874 (Cy-*O*-acetylserine thiol lyase, *Leucaena leucocephala*).

Acknowledgements We are grateful to Dr. Shinichi Gima of the Instrumental Research Center, University of the Ryukyus, and Dr. Michael Chandro Roy of the Okinawa Institute of Science and Technology for providing technical assistance during the LC–MS/MS analyses. We sincerely thank to Dr. Rafiq Islam (Professor, Department of Natural Sciences, Northwest Missouri State University) for useful discussion and necessary corrections of our manuscript.

References

Birke H, De Kok LJ, Wirtz M, Hell R (2015) The role of compartment-specific cysteine synthesis for sulfur homeostasis during H_2S exposure in Arabidopsis. Plant Cell Physiol 56:358–367

Bonner ER, Cahoon RE, Knapke SM, Jez JM (2005) Molecular basis of cysteine biosynthesis in plants: structural and functional analysis of *O*-acetylserine sulfhydrylase from *Arabidopsis thaliana*. J Biol Chem 280:38803–38813

Buchner P, Takahashi H, Hawkesford MJ (2004) Plant sulphate transporters: co-ordination of uptake, intracellular and long-distance transport. J Exp Bot 55:1765–1773

Burkhard P, Tai CH, Jansonius JN, Cook PF (2000) Identification of an allosteric anion-binding site on *O*-acetylserine sulfhydrylase: structure of the enzyme with chloride bound. J Mol Biol 303:279–286

Campanini B, Speroni F, Salsi E, Cook PF, Roderick SL, Huang B, Bettati S, Mozzarelli A (2005) Interaction of serine acetyltransferase with *O*-acetylserine sulfhydrylase active site: evidence from fluorescence spectroscopy. Protein Sci Publ Protein Soc 14:2115–2124

Claus MT, Zocher GE, Maier TH, Schulz GE (2005) Structure of the *O*-acetylserine sulfhydrylase isoenzyme CysM from *Escherichia coli*. BioChemistry 44:8620–8626

Droux M, Ruffet ML, Douce R, Job D (1998) Interactions between serine acetyltransferase and *O*-acetylserine (thiol) lyase in higher plants–structural and kinetic properties of the free and bound enzymes. Eur J Biochem 255:235–245

Eliot AC, Kirsch JF (2004) Pyridoxal phosphate enzymes: mechanistic, structural, and evolutionary considerations. Annu Rev Biochem 73:383–415

Feldman-Salit A, Wirtz M, Hell R, Wade RC (2009) A mechanistic model of the cysteine synthase complex. J Mol Biol 386:37–59

Felsenstein J (1985) Confidence limits on phylogenies: an approach using the bootstrap. Evolution Int J org Evolut 39:783–791

Gaitonde MK (1967) A spectrophotometric method for the direct determination of cysteine in the presence of other naturally occurring amino acids. Biochem J 104:627–633

Haas FH, Heeg C, Queiroz R, Bauer A, Wirtz M, Hell R (2008) Mitochondrial serine acetyltransferase functions as a pacemaker of cysteine synthesis in plant cells. Plant Physiol 148:1055–1067

Heeg C, Kruse C, Jost R, Gutensohn M, Ruppert T, Wirtz M, Hell R (2008) Analysis of the Arabidopsis *O*-acetylserine(thiol)lyase gene family demonstrates compartment-specific differences in the regulation of cysteine synthesis. Plant Cell 20:168–185

Hell R, Wirtz M (2008) Metabolism of cysteine in plants and phototrophic bacteria. In: Hell R, Dahl C, Knaff D, Leustek T (eds) Sulfur metabolism in phototrophic organisms. Springer Netherlands, Dordrecht, pp 59–91

Ikegami F, Mizuno M, Kihara M, Murakoshi I (1990) Enzymatic synthesis of the thyrotoxic amino acid mimosine by cysteine synthase. Phytochemistry 29:3461–3465

Inoue K, Noji M, Saito K (1999) Determination of the sites required for the allosteric inhibition of serine acetyltransferase by L-cysteine in plants. Eur J Biochem 266:220–227

Ishikawa T, Ishikura T, Kuwata K (2009) Theoretical study of the prion protein based on the fragment molecular orbital method. J Comput Chem 30:2594–2601

Kitaura K, Ikeo E, Asada T, Nakano T, Uebayasi M (1999a) Fragment molecular orbital method: an approximate computational method for large molecules. Chem Phys Lett 313:701–706

Kitaura K, Sawai T, Asada T, Nakano T, Uebayasi M (1999b) Pair interaction molecular orbital method: an approximate computational method for molecular interactions. Chem Phys Lett 312:319–324

Krueger S, Niehl A, Lopez Martin MC, Steinhauser D, Donath A, Hildebrandt T, Romero LC, Hoefgen R, Gotor C, Hesse H (2009) Analysis of cytosolic and plastidic serine acetyltransferase mutants and subcellular metabolite distributions suggests interplay of the cellular compartments for cysteine biosynthesis in Arabidopsis. Plant Cell Environ 32:349–367

Kumar S, Stecher G, Tamura K (2016) MEGA7: molecular evolutionary genetics analysis version 7.0 for bigger datasets. Mol Biol Evol 33:1870–1874

Kumaran S, Jez JM (2007) Thermodynamics of the interaction between *O*-acetylserine sulfhydrylase and the C-terminus of serine acetyltransferase. BioChemistry 46:5586–5594

Kuske CR, Ticknor LO, Guzman E, Gurley LR, Valdez JG, Thompson ME, Jackson PJ (1994) Purification and characterization of *O*-acetylserine sulfhydrylase isoenzymes from *Datura innoxia*. J Biol Chem 269:6223–6232

Lafaye A, Junot C, Pereira Y, Lagniel G, Tabet JC, Ezan E, Labarre J (2005) Combined proteome and metabolite-profiling analyses reveal surprising insights into yeast sulfur metabolism. J Biol Chem 280:24723–24730

Murakoshi I, Kuramoto H, Haginiwa J, Fowden L (1972) The enzymic synthesis of β-substituted alanines. Phytochemistry 11:177–182

Na G, Salt DE (2011) The role of sulfur assimilation and sulfur-containing compounds in trace element homeostasis in plants. Environ Exp Bot 72:18–25

Ngo H, Harris R, Kimmich N, Casino P, Niks D, Blumenstein L, Barends TR, Kulik V, Weyand M, Schlichting I, Dunn MF (2007)

Synthesis and characterization of allosteric probes of substrate channeling in the tryptophan synthase bienzyme complex. Biochemistry 46:7713–7727

Noji M, Inoue K, Kimura N, Gouda A, Saito K (1998) Isoform-dependent differences in feedback regulation and subcellular localization of serine acetyltransferase involved in cysteine biosynthesis from *Arabidopsis thaliana*. J Biol Chem 273:32739–32745

Pilon-Smits EAH, Pilon M (2006) Sulfur Metabolism in Plastids. In: Wise RR, Hoober JK (eds) The structure and function of plastids. Springer Netherlands, Dordrecht, pp 387–402

Ponder JW, Case DA (2003) Force fields for protein simulations. Adv Protein Chem 66:27–85

Renosto F, Patel HC, Martin RL, Thomassian C, Zimmerman G, Segel IH (1993) ATP sulfurylase from higher plants: kinetic and structural characterization of the chloroplast and cytosol enzymes from spinach leaf. Arch Biochem Biophys 307:272–285

Saito K (2000) Regulation of sulfate transport and synthesis of sulfur-containing amino acids. Curr Opin Plant Biol 3:188–195

Saito K (2004) Sulfur assimilatory metabolism. The long and smelling road. Plant Physiol 136:2443–2450

Saito K, Tatsuguchi K, Takagi Y, Murakoshi I (1994) Isolation and characterization of cDNA that encodes a putative mitochondrion-localizing isoform of cysteine synthase (*O*-acetylserine(thiol)-lyase) from *Spinacia oleracea*. J Biol Chem 269:28187–28192

Saitou N, Nei M (1987) The neighbor-joining method: a new method for reconstructing phylogenetic trees. Mol Biol Evol 4:406–425

Scharer MA, Eliot AC, Grutter MG, Capitani G (2011) Structural basis for reduced activity of 1-aminocyclopropane-1-carboxylate synthase affected by a mutation linked to andromonoecy. FEBS lett 585:111–114

Simanshu DK, Savithri HS, Murthy MR (2006) Crystal structures of *Salmonella typhimurium* biodegradative threonine deaminase and its complex with CMP provide structural insights into ligand-induced oligomerization and enzyme activation. J Biol Chem 281:39630–39641

Tai C-H, Cook PF (2006) *O*-acetylserine sulfhydrylase. Adv Enzym Relat Areas Mol Biol 74:185–234

Takahashi H, Kopriva S, Giordano M, Saito K, Hell R (2011) Sulfur assimilation in photosynthetic organisms: molecular functions and regulations of transporters and assimilatory enzymes. Annu Rev Plant Biol 62:157–184

Warrilow AGS, Hawkesford MJ (2000) Cysteine synthase (*O*-acetylserine (thiol) lyase) substrate specificities classify the mitochondrial isoform as a cyanoalanine synthase. J Exp Bot 51:985–993

Watanabe M, Mochida K, Kato T, Tabata S, Yoshimoto N, Noji M, Saito K (2008) Comparative genomics and reverse genetics analysis reveal indispensable functions of the serine acetyltransferase gene family in Arabidopsis. Plant Cell 20:2484–2496

Wirtz M, Hell R (2006) Functional analysis of the cysteine synthase protein complex from plants: structural, biochemical and regulatory properties. J Plant Physiol 163:273–286

Wirtz M, Droux M, Hell R (2004) O-acetylserine (thiol) lyase: an enigmatic enzyme of plant cysteine biosynthesis revisited in *Arabidopsis thaliana*. J Exp Bot 55:1785–1798

Wirtz M, Birke H, Heeg C, Müller C, Hosp F, Throm C, König S, Feldman-Salit A, Rippe K, Petersen G, Wade RC, Rybin V, Scheffzek K, Hell R (2010a) Structure and function of the hetero-oligomeric cysteine synthase complex in plants. J Biol Chem 285:32810–32817

Wirtz M, Heeg C, Samami AA, Ruppert T, Hell R (2010b) Enzymes of cysteine synthesis show extensive and conserved modifications patterns that include N(α)-terminal acetylation. Amino Acids 39:1077–1086

Wirtz M, Beard KFM, Lee CP, Boltz A, Schwarzlaender M, Fuchs C, Meyer AJ, Heeg C, Sweetlove LJ, Ratcliffe RG, Hell R (2012) Mitochondrial cysteine synthase complex regulates *O*-acetylserine biosynthesis in plants. J Biol Chem 287:27941–27947

Yafuso JT, Negi VS, Bingham JP, Borthakur D (2014) An *O*-acetylserine (thiol) lyase from *Leucaena leucocephala* is a cysteine synthase but not a mimosine synthase. Appl Biochem Biotechnol 173:1157–1168

Yi H, Juergens M, Jez JM (2012) Structure of soybean β-cyanoalanine synthase and the molecular basis for cyanide detoxification in plants. Plant Cell 24:2696–2706

Zuckerkandl E, Pauling L (1965) Evolutionary divergence and convergence in proteins. Academic Press, New York